Impact of electron collisions on the skin effect in a photoionized inert gas plasma

K. Yu. Vagin, T. V. Mamontova, and S. A. Uryupin*
Lebedev Physical Institute, Russian Academy of Science, Moscow 119991, Russia

(Received 29 April 2020; accepted 20 July 2020; published 6 August 2020)

The interaction of monochromatic electromagnetic radiation with a photoionized plasma formed during multiphoton ionization of inert gas atoms is studied. It is shown how electron collisions with neutral atoms affect the surface impedance and absorption coefficient. The possibility of a significant absorption coefficient growth in the regimes of high-frequency and normal skin effects due to the manifestation of the Ramsauer-Townsend effect was revealed. The conditions under which the interaction of test low-frequency radiation with a photoionized inert gas plasma is similar to the interaction with a dielectric with a permittivity having a small imaginary part are established.

DOI: 10.1103/PhysRevA.102.023105

I. INTRODUCTION

A photoionized plasma with a nonequilibrium electron distribution that differs qualitatively from Maxwellian is formed during ionization of inert gas atoms by a short pulse of laser radiation. A number of papers have been devoted to studying the characteristics of the angular [1–7] and energy [1,6–10] distribution of photoelectrons, as well as their spin polarization [11–13] in various ionization modes of inert gas atoms. The nonequilibrium distribution of photoelectrons is approximated by different functions. The anisotropic bi-Maxwell distribution [14,15] or toroidal distribution [14,16,17] is often used to describe photoelectrons in a tunnel regime of atom ionization, depending on the polarization of ionizing radiation. In the case of multiphoton or above-threshold ionization the distribution of photoelectrons is approximated by the one- or multipeak distributions [18,19], including the anisotropic ones [20]. The patterns of the plasma photoelectron distribution significantly affect the ionized gas properties. In particular, the presence of the distribution function anisotropy leads to the development of aperiodic instabilities, accompanied by the generation of a magnetic field [21,22] or a quasipotential field [23,24]. There is a possibility of electromagnetic radiation pulses amplification in their interaction with an unstable anisotropic photoionized plasma [15,25].

In weakly ionized plasma, the elastic scattering of electrons by neutral atoms leads to isotropization of the distribution function. The photoelectron distribution over energy still remains nonequilibrium for a relatively long time. For a plasma formed during above-threshold ionization, the energy photoelectron spectrum consists of a set of individual peaks, each of which corresponds to the absorption of a certain number of photons (see, e.g., Refs. [8,26]). Longitudinal waves with a linear dispersion law and a group velocity comparable to the characteristic velocity of photoelectrons can exist in an isotropic photoionized plasma [19,27]. The number of waves is greater the greater the number of peaks in the distribution function [19]. The new physical properties appear due to the presence of the Ramsauer-Townsend effect in the photoionized inert gas plasma [28–30]. The peculiar behavior of the photoelectron scattering cross section corresponding to this effect leads to the possibility of amplification of low-frequency radiation pulses [18,31].

The present paper considers the specific features of the monochromatic electromagnetic field penetration into a plasma formed by multiphoton ionization of inert gases, continuing the study of the unusual properties of a nonequilibrium photoionized plasma. The conditions when elastic electron collisions with neutral atoms led to isotropization of the photoelectrons distribution, but the energy distribution remained highly nonequilibrium, are considered. Particular attention is paid to the study of the effects associated with the electron scattering cross section minimum on the neutral atoms of inert gases. The field penetration is studied in the regimes of high-frequency and normal skin effects, as well as in the case when the properties of the photoionized plasma are similar to the properties of a dielectric. Expressions for the surface impedance and absorption coefficient are obtained for different ratios between the plasma frequency and the incident radiation frequency. It is shown that in the regimes of normal and high-frequency skin effects, the presence of a positive derivative of the collision frequency at a point corresponding to the characteristic speed of photoelectrons leads to an increase in absorption by several times. For not abnormally small collision frequencies of electrons, collisional absorption is dominant in the whole range of considered radiation frequencies. The contribution to the absorption from the Cherenkov interaction of electrons with the field is relatively small.

II. INERT GAS PHOTOELECTRONS

Let us consider a weakly ionized plasma formed during the multiphoton ionization of inert gas atoms by a short laser pulse (see, e.g., Refs. [8,9,18]). In such a plasma, the energy

*uryupin@sci.lebedev.ru

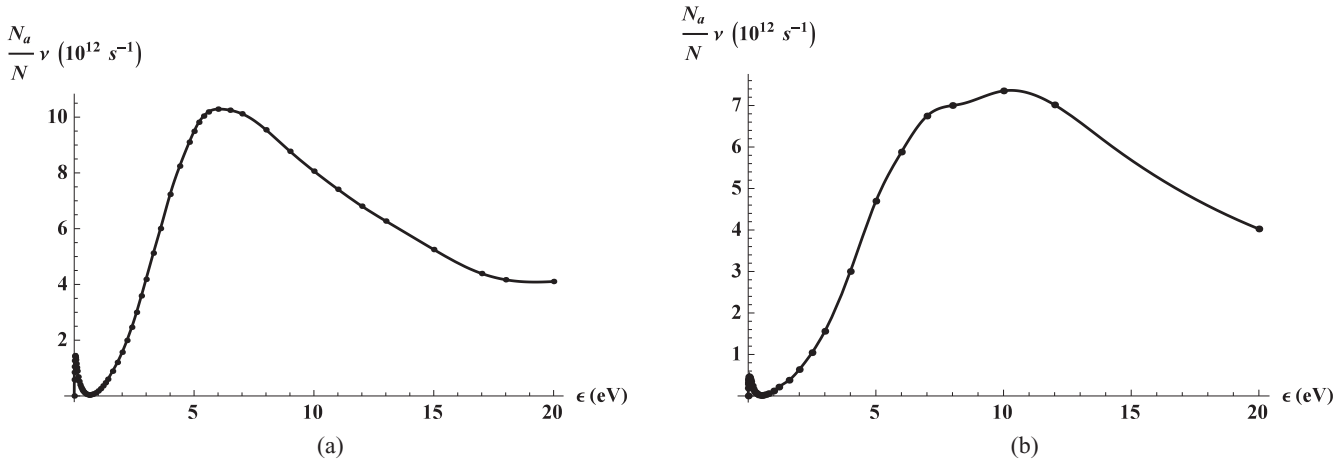

FIG. 1. Dependence of the collision frequency of photoelectrons with (a) xenon neutral atoms and (b) krypton neutral atoms on the average photoelectron energy ϵ. $N_a = 2.5 \times 10^{19}$ cm^{-3} is the concentration of atoms at atmospheric pressure.

photoelectron distribution has the form of one narrow peak corresponding to the absorption of the minimum required number K of photons to overcome the ionization threshold determined by the ionization potential of the atom E_i. The maximum position of the photoelectron distribution function corresponds to the energy ϵ_0, determined according to the formula for the multiphoton photoelectric effect $\epsilon_0 = K\hbar\Omega - E_i$ and having a value of the order of several eV. Here, $\hbar$ is the Planck constant and Ω is the frequency of ionizing radiation.

In the case of linear polarization of the ionizing radiation field, an anisotropic distribution is formed, in which the electron velocities are mainly oriented along and against the vector of field strength. However, under conditions of weak ionization of a not abnormally rarefied gas, scattering of photoelectrons by neutral atoms leads to a rapid relaxation of their momentum. Therefore, it is justified to use the isotropic velocity distribution function, which remains nonequilibrium and corresponds to the peaklike energy spectrum at times exceeding the inverse effective frequency of photoelectron elastic collisions. Further we use the distribution function corresponding to the "cold" plasma model,

$$f(v) = \frac{n}{4\pi v_0^2}\,\delta(v - v_0), \tag{1}$$

when studying the penetration of an electromagnetic field into a photoionized plasma, where n is the photoelectron density, $v_0 = \sqrt{2\epsilon_0/m}$, and m is the electron mass. The spread in photoelectron energies is considered insignificant in such a model. The nonequilibrium distribution (1) relaxes to the Maxwell distribution due to electron-electron collisions and quasielastic collisions of photoelectrons with neutral atoms at significantly longer times. Further we will consider the effect of radiation, the frequency of which is much greater than the inverse time of relaxation of the distribution function (1).

Further consideration will be carried out in relation to the plasma obtained by ionization of inert gas atoms. Under typical conditions of multiphoton ionization, a weakly ionized plasma, in which the energy corresponding to the peak in the photoelectron distribution does not exceed several eV, is formed. In the case of monoatomic inert gases, the lower excitation threshold of intra-atomic electronic states in electron and atom collisions is noticeably higher. For example, for the Xe atom, such a threshold exceeds 8 eV, and for the Kr atom it exceeds 10 eV. Therefore, photoelectron scattering is determined mainly by elastic collisions with neutral atoms. A characteristic feature of the elastic electrons scattering by inert gas atoms is the presence of a minimum scattering cross section in the energy region slightly lower than 1 eV [28–30] called the Ramsauer-Townsend effect. In particular, for xenon the minimum takes place near the energy $\epsilon = mv^2/2 \sim 0.6$ eV, and for krypton $\epsilon \sim 0.5$ eV. Further we will use the photoelectron collision frequency with neutral atoms, defined as $\nu(v) = N\sigma_{\rm tr}(v)v$, where N is the concentration of neutral atoms and $\sigma_{\rm tr}(v)$ is the transport cross section for electron scattering by neutral atoms, which depends on the photoelectrons speed. Using the values of the transport cross section for elastic electron scattering by atoms Xe given in [32], for $\nu(v)$ we have the dependence shown in Fig. 1(a). Points on a curve in Fig. 1(a) correspond to the experimental data of [32]. A similar dependence of the collision frequency on energy in the photoelectron scattering by krypton atoms is shown in Fig. 1(b). The experimental data for krypton is taken from [33]. In xenon, the collision frequency increases in the energy range $\epsilon \sim$ (0.6–6) eV and in krypton it increases in the range $\epsilon \sim$ (0.5–10) eV. Further it will be shown that the presence of such an interval is responsible for enhancing the incident electromagnetic wave absorption.

III. INTERACTION OF AN ELECTROMAGNETIC WAVE WITH A SEMIBOUNDED PLASMA

Let us consider the normal incidence of a monochromatic electromagnetic wave $\boldsymbol{E}(z,t) = (1/2)(E_0, 0, 0)\exp[-i\omega(t - z/c)] + \text{c.c.}$ to a photoionized plasma occupying the half-space $z > 0$ and having a photoelectron distribution of the form (1), where c is the speed of light and ω is the frequency. Such an electromagnetic wave generates in the plasma an electric field directed along the ox of the form $(1/2)\boldsymbol{E}(z)\exp(-i\omega t) + \text{c.c.}$ and leads to a small perturbation of the photoelectron distribution function over velocities of the form $(1/2)\,\delta f(\mathbf{v}, z)\exp(-i\omega t) + \text{c.c.}$ We use the linearized kinetic equation with the collision

integral, which describes relaxation along the directions of the photoelectron momentum without changing their energy, to determine $\delta f(\mathbf{v}, z)$

$$-i\omega\delta f(\mathbf{v},z)+v_z\frac{\partial}{\partial z}\delta f(\mathbf{v},z)+\frac{ev_xE(z)}{mv}\frac{\partial f_0(v)}{\partial v} = -\nu(v)\left[\delta f(\mathbf{v},z)-\int\frac{d\Omega}{4\pi}\delta f(\mathbf{v},z)\right], \quad (2)$$

where e is the electron charge and $d\Omega$ is the solid angle element.

Following [34], after the joint solution of (2) and the Maxwell system of equations, in the case of specular reflection of electrons from the plasma boundary $z = 0$, for the field in the plasma we have

$$E(z)=\frac{2E_0}{1+Z(\omega)}\frac{i\omega}{c}\int_{-\infty}^{+\infty}\frac{dk}{\pi}\frac{\exp(ikz)}{\varepsilon_{\rm tr}(\omega,k)\,\omega^2/c^2-k^2}, \quad (3)$$

where the transverse permittivity of the plasma has the form

$$\varepsilon_{\rm tr}(\omega,k)=1+\frac{4\pi e^2}{m\omega}\int\frac{v_x^2\,d\mathbf{v}}{\omega+i\nu(v)-kv_z}\frac{\partial f_0(v)}{v\,\partial v}. \quad (4)$$

The expression (4) differs from that used previously [34] by the dependence of the collision frequency on the electron velocity, which allows one to take into account the Ramsauer-Townsend effect. For a "cold" photoionized plasma with the photoelectron distribution function (1) the transverse permittivity (4) has the form

$$\varepsilon_{\rm tr}(\omega,k)=1-\frac{\omega_L^2}{\omega k v_0}\left[\operatorname{arcth}\left(\frac{kv_0}{\omega+i\nu}\right)\times\left(1-\alpha\frac{i\nu(\omega+i\nu)}{k^2v_0^2}\right)+\alpha\frac{i\nu}{kv_0}\right], \quad (5)$$

where $\omega_L=\sqrt{4\pi ne^2/m}$ is the Langmuir electron frequency, and $\nu\equiv\nu(v_0)$, $\alpha=\partial\,\ln\nu/\partial\,\ln v_0$ is the value determined by the average photoelectron energy and the energy dependence type of the scattering transport cross section. The arctanh(u) is the inverse hyperbolic tangent of a complex argument defined according to 4.6.3 from [35]

$$\operatorname{arctanh}(u)=\int_0^u\frac{ds}{1-s^2}, \quad (6)$$

where the integration path does not intersect the real axis from $-\infty$ to -1 and from 1 to $+\infty$. The function $Z\equiv Z(\omega)=i\omega E(+0)/cE'(+0)$ in (3) represents the surface plasma impedance. The relation between the surface impedance and the field at the plasma boundary has the form $Z/(1+Z)=E(+0)/2E_0$. The surface impedance determines the absorption coefficient $A(\omega)$ according to the relation

$$A(\omega)=1-\left|\frac{Z(\omega)-1}{Z(\omega)+1}\right|^2. \quad (7)$$

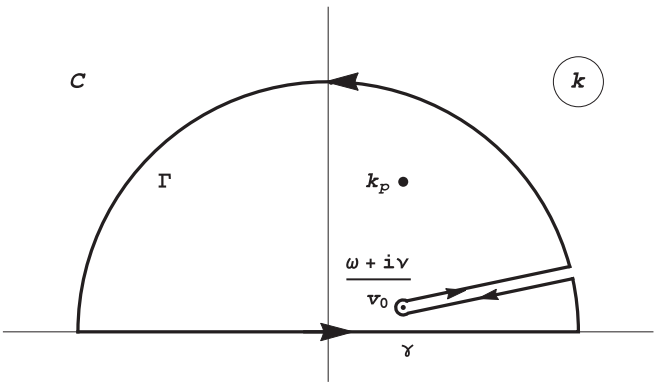

FIG. 2. Integration contour for the electric field inside the plasma.

IV. ELECTRIC FIELD IN PHOTOIONIZED PLASMA

The electric field in the plasma (3) is determined by the integral over the real variable k, corresponding to the inverse Fourier transform. We continue analytically the integrands in the upper half-plane of the complex variable k to calculate it. Taking into account properties of the function (6) in the complex plane [35], we use the contour C shown in Fig. 2 to calculate the integral (3). In the plane of the variable k the cut starts from the point $k=(\omega+i\nu)/v_0$ and goes to ∞ along the ray coming out of the origin at the angle $\arctan(\nu/\omega)$ to the real axis k. The contribution from the integrals over a circle of infinitesimal radius centered at $(\omega+i\nu)/v_0$ and a semicircle of infinitely large radius in the upper half-plane are 0. Then, according to the Cauchy theorem, the electric field in the plasma (3) can be represented as the sum of two terms:

$$E(z)=E_1(z)+E_2(z). \quad (8)$$

Here, the first term $E_1(z)$ is related to the contribution to the integral from the pole of the integrand (3) inside the integration contour C. The second term $E_2(z)$ corresponds to the total contribution from the integrals along the banks of the cut, taken with the opposite sign. The solution of the transcendental equation

$$\varepsilon_{\rm tr}(\omega,k_p)-\frac{k_p^2c^2}{\omega^2}=0, \quad (9)$$

where $\varepsilon_{\rm tr}(\omega,k)$ is defined by the expression (5), allows us to find the pole position $k_p\equiv k_p(\omega)$ of the integrand (3). Using a numerical analysis of Eq. (9) it was found that the integrand (3) in the upper half-plane of the complex variable k has a single pole, the real part of which is positive. In this case, the contribution to the field $E_1(z)$ can be represented as

$$E_1(z)=-\frac{4E_0}{1+Z(\omega)}\frac{c}{\omega}\left[\left.\frac{\partial(\varepsilon_{\rm tr}(\omega,k)-k^2c^2/\omega^2)}{\partial k}\right|_{k=k_p}\right]^{-1}\exp[ik_p(\omega)z]. \quad (10)$$

To find $E_2(z)$ we use the properties of the function (6) in (5) on the banks of the cut. By changing the variable $k = t \cdot (\omega + i\nu)/v_0$ we get the integrals along the real axis, where the new variable varies within $1 < t < \infty$. There are the relations along the banks of the cut

$$\operatorname{arctanh}(t \pm i\,0) = \pm i\frac{\pi}{2} + \operatorname{arccoth}(t), \qquad t > 1,$$

where the upper (lower) sign corresponds to the upper (lower) bank of the cut on the contour selected for integration. Given the above, we have for $E_2(z)$

$$E_2(z) = \frac{2E_0}{1+Z}\frac{c}{v_0}\left(\frac{\omega+i\nu}{\omega_L}\right)^2 \int_1^\infty dt\, t\left(1 - i\frac{\alpha\nu}{\omega+i\nu}\frac{1}{t^2}\right)\exp\left[\frac{i\omega-\nu}{v_0}zt\right]\left\{\left[\frac{\omega(\omega+i\nu)}{\omega_L^2}t\right.\right.$$
$$\left.\times\left[\frac{c^2}{v_0^2}\left(\frac{\omega+i\nu}{\omega}\right)^2 t^2 - 1\right] + \operatorname{arccoth}(t)\left(1 - i\frac{\alpha\nu}{\omega+i\nu}\frac{1}{t^2}\right) - i\frac{\alpha\nu}{\omega+i\nu}\frac{1}{t}\right]^2 + \frac{\pi^2}{4}\left(1 - i\frac{\alpha\nu}{\omega+i\nu}\frac{1}{t^2}\right)^2\left.\right\}^{-1}. \quad (11)$$

The ratios (10) and (11) form the basis for further analysis of the field in the plasma.

V. HIGH-FREQUENCY SKIN EFFECT

In a rarefied plasma, the photoelectron collision frequencies are relatively small and the conditions when $\omega \gg \nu$ are of interest. The influence of electron motion on the field penetration under such conditions is most pronounced in the anomalous skin-effect mode when $v_0 > c\omega/\omega_L$. This mode is described in [36]. The paper [36] also considers high-frequency skin effect, when $\omega > \omega_L v_0/c$. However, in [36] we completely neglect the impact of collisions. In this section, in the development of [36] we study the collision effect on the field penetration in the high-frequency skin effect when

$$\omega \gg \nu, kv_0. \quad (12)$$

In this mode, the solution of Eq. (9) lies in the small wave number region for which the inequality $|k_p|v_0 \ll \omega$ holds and the transverse permittivity (5) has the form

$$\varepsilon_{\rm tr}(\omega, k) = 1 - \frac{\omega_L^2}{\omega^2}\left[1 + \frac{k^2 v_0^2}{3\,\omega^2} - i\left(\frac{\alpha}{3}+1\right)\frac{\nu}{\omega}\right]. \quad (13)$$

Moreover, the solution of Eq. (9), which determines the pole of the integrand (3), has the form

$$k_p^2(\omega)c^2 = \left(\omega^2 - \omega_L^2\right)\left(1 - \frac{v_0^2}{3c^2}\frac{\omega_L^2}{\omega^2}\right) + i\left(\frac{\alpha}{3}+1\right)\frac{\nu}{\omega}\,\omega_L^2. \quad (14)$$

In the framework of the inequality (12) for the field $E_1(z)$ (10) we find

$$E_1(z) = \frac{2E_0}{1+Z(\omega)}\frac{\omega}{k_p(\omega)c}\left(1 - \frac{v_0^2}{3c^2}\frac{\omega_L^2}{\omega^2}\right) \times \exp[ik_p(\omega)z]. \quad (15)$$

In turn, the integral (11) that defines the field $E_2(z)$ contains an oscillating function of the coordinate z and, on spatial scales exceeding the distance traveled by the photoelectron during the change in the field $z > v_0/\omega$, the function $E_2(z)$ significantly decreases. Consider also that under the conditions (12) the main contribution to the integral (11) is determined by the values of the integration variable near the lower limit. For the maximum value $E_2(z)$, which is reached near the plasma boundary, we have the expression

$$E_2(+0) = \frac{1}{2}\frac{E_0}{1+Z(\omega)}\frac{v_0^3\omega_L^2}{c^3\omega^2}, \quad (16)$$

which is much smaller than $E_1(+0)$. Thus, under the conditions of the high-frequency skin effect (12), the field penetrating into the plasma (3) is mainly determined by the contribution (10) from the pole (14) in the upper half-plane of the complex wave number $E(z) \approx E_1(z)$ (see Fig. 3). The presence of small oscillations in the inset to Fig. 3 is due to contribution from the banks of the cut. The negligible under the conditions of the high-frequency skin-effect Cherenkov absorption is connected with precisely these oscillations. Using the expressions (15) and (16), we obtain the surface impedance of the photoionized plasma in the frequency range (12)

$$Z(\omega) = \frac{\omega}{k_p(\omega)c}\left(1 - \frac{v_0^2}{3c^2}\frac{\omega_L^2}{\omega^2}\right) + \frac{v_0^3}{4\,c^3}\frac{\omega_L^2}{\omega^2}. \quad (17)$$

A. Range of frequencies less than Langmuir frequency

We consider three limiting cases. If the frequency of the incident wave on the plasma does not exceed the Langmuir

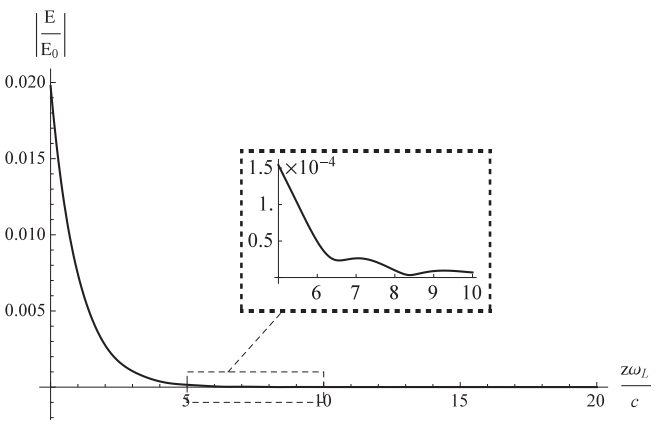

FIG. 3. Dependence of the field absolute value in the plasma on the distance to the plasma boundary with parameters $c\omega/\omega_L v_0 = 3$ and $c\nu/\omega_L v_0 = 0.01$.

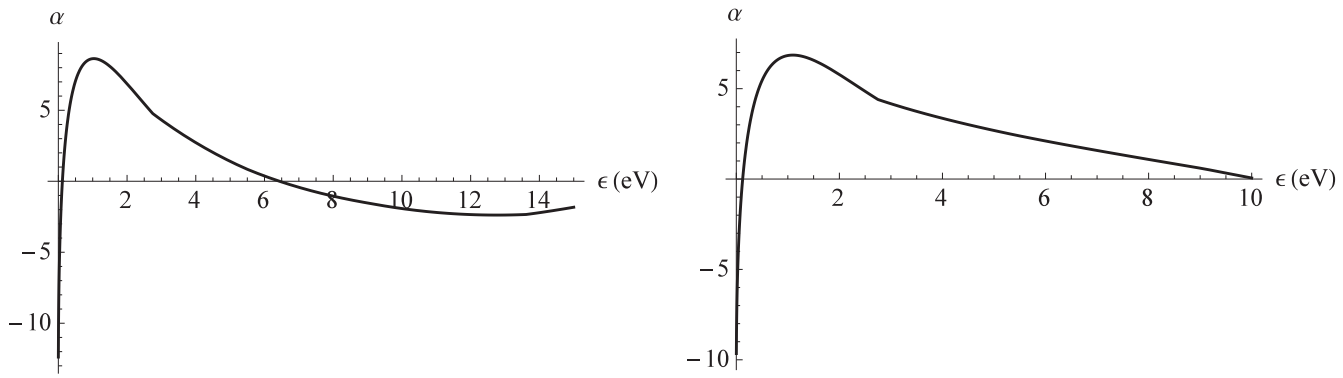

FIG. 4. Dependence of the parameter α on the average photoelectron energy ϵ for (a) Xe and for (b) Kr.

frequency and is not too close to it

$$\omega_L - \omega \gg \frac{\nu}{4}\left(\frac{\alpha}{3}+1\right), \tag{18}$$

for the pole (14), which determines the spatial structure of the field penetrating into the plasma, we obtain

$$k_p(\omega) \equiv k_p'(\omega) + i\,k_p''(\omega) \approx \frac{\omega_L^2}{2\omega c}\left(\frac{\alpha}{3}+1\right) \times \frac{\nu}{\sqrt{\omega_L^2-\omega^2}} + i\frac{\sqrt{\omega_L^2-\omega^2}}{c}\left(1-\frac{v_0^2}{6c^2}\frac{\omega_L^2}{\omega^2}\right). \tag{19}$$

Under the inequalities (12) and (18) the relation $k_p'(\omega) \ll k_p''(\omega)$ holds, according to which the decrease in the amplitude of the electric field occurs at distances $\sim 1/k_p''(\omega)$, which is much smaller than the spatial scale of the oscillations of the field $2\pi/k_p'(\omega)$. In this case, the characteristic scale of such oscillations varies inversely with the collision frequency of photoelectrons. In the same limit, from the expression (17) we find the surface impedance

$$Z(\omega) = -i\frac{\omega}{\sqrt{\omega_L^2-\omega^2}}\left(1-\frac{v_0^2}{6c^2}\frac{\omega_L^2}{\omega^2}\right) + \left(\frac{\alpha}{3}+1\right)\frac{\nu\,\omega_L^2}{2\left(\omega_L^2-\omega^2\right)^{3/2}} + \frac{v_0^3\omega_L^2}{4c^3\omega^2}. \tag{20}$$

Note that the contribution to the field absorption is made only by the real terms in the expression (20). Substituting (20) into the absorption coefficient (7), for frequencies (18) not too close to the plasma we find

$$A(\omega) \approx \left(\frac{\alpha}{3}+1\right)\frac{2\nu}{\sqrt{\omega_L^2-\omega^2}} + \frac{v_0^3}{c^3}\left(\frac{\omega_L^2}{\omega^2}-1\right) \ll 1. \tag{21}$$

In accordance with the inequality (12) and the formula (19), the relations (20) and (21) hold for

$$\omega \gg \nu,\ (v_0/c)\sqrt{\omega_L^2-\omega^2} \tag{22}$$

and the inequality (18). The absorption coefficient (21) takes into account two different absorption mechanisms. The first of them is related to electron collisions and is described by the proportional ν term in (21). This term behaves as an increasing function of the incident field frequency and differs from the known one [34] by the parameter α, which takes into account the dependence of the collision frequency on a velocity due to the Ramsauer-Townsend effect. The energy dependencies of α for xenon and krypton are shown in Fig. 4. To obtain the graphs in Figs. 4(a) and 4(b) we used the energy dependencies of the collision frequency given in Figs. 1(a) and 1(b), respectively. In the case of a Xe photoionized plasma [18], for which $\epsilon_0 = 2.87$ eV, the parameter $\alpha/3 \approx 1.5 > 1$. That is why taking into account the Ramsauer-Townsend effect leads to an increase in absorption by 2.5 times.

The second term in (21) describes collisionless absorption arising due to weak spatial dispersion, which decreases with increasing field frequency. The two terms in the absorption coefficient $A(\omega)$ are comparable when $2\nu(\alpha/3+1) \sim (v_0/c)^3(\omega_L^2-\omega^2)^{3/2}\omega^{-2}$. According to Figs. 4(a) for Xe and 4(b) for Kr, the parameter $(\alpha/3+1)$ in the energy range of interest from 0.5 to 10 eV varies in the range from 1 to 4 for Xe and from 1 to 3 for Kr. Therefore, under the conditions of applicability of the formula (21) [see the inequality (22)], the absorption due to collisions becomes the main one at frequencies ν noticeably lower than ω and increases with increasing ν.

B. Range of frequencies close to Langmuir frequency

In the limit, when the incident wave frequency is close to the Langmuir frequency and the inequality

$$|\omega - \omega_L| \ll \frac{\nu}{4}\left(\frac{\alpha}{3}+1\right) \tag{23}$$

holds, from (14) we obtain the following expression for the wave number, which determines the position of the pole:

$$k_p(\omega \approx \omega_L) = \frac{1+i}{\sqrt{2}}\frac{\sqrt{\omega_L\,\nu\,(\alpha/3+1)}}{c}. \tag{24}$$

According to (24) $k_p'(\omega_L) = k_p''(\omega_L)$ and the field decreases with increasing z at the same distances as its spatial oscillations. In this case, the effective depth of the field penetration into the plasma is inversely proportional to $\sqrt{\nu}$ and greater than in the case of lower field frequencies (18). From (17) we find the surface impedance of the photoionized plasma when

the frequency of the incident wave is close to the Langmuir frequency

$$Z(\omega \approx \omega_L) = \frac{1-i}{\sqrt{2}}\sqrt{\frac{\omega_L}{\nu}\frac{1}{\alpha/3+1}}. \tag{25}$$

Corrections of order v_0^2/c^2 are omitted in the expression (25) and everywhere below. This approach is justified, since for typical values of photoelectron energy for multiphoton ionization $\epsilon_0 \sim 1$ eV the parameter $v_0^2/c^2 \sim 10^{-6} \ll 1$. The absorption coefficient (7) corresponding to the impedance (25) is due to electron collisions and has the form

$$A(\omega \approx \omega_L) \approx \sqrt{\frac{8\,\nu}{\omega_L}\left(\frac{\alpha}{3}+1\right)} \ll 1. \tag{26}$$

A comparison of the expressions (21) and (26) demonstrates that, within the inequality (12), with increasing frequency ω of the wave incident on the plasma and especially when it approaches ω_L, the absorption of the wave is enhanced and accompanied by an increase in the penetration depth into the plasma. For not abnormally low collision frequencies in the entire region of the high-frequency skin effect, the dominant absorption mechanism is electron collisions with gas atoms, while the collisionless mechanism of energy transfer from the wave to the photoelectrons associated with spatial dispersion leads only to small corrections in the absorption coefficient.

C. High-frequency range

With a noticeable excess of the wave incident frequency over the Langmuir frequency, when

$$\omega - \omega_L \gg \frac{\nu}{4}\left(\frac{\alpha}{3}+1\right), \tag{27}$$

from (14) we get

$$k_p(\omega) \equiv k_p'(\omega) + i\,k_p''(\omega) \approx \frac{\sqrt{\omega^2-\omega_L^2}}{c} + i\frac{\omega_L^2}{2\omega c}\left(\frac{\alpha}{3}+1\right)\frac{\nu}{\sqrt{\omega^2-\omega_L^2}}. \tag{28}$$

Thus, in the frequency range (27), the expression (15) describes a transverse electromagnetic wave propagating deep into the plasma with a wavelength $2\pi/k_p'(\omega) = 2\pi c/\sqrt{\omega^2-\omega_L^2}$ much smaller than the characteristic distance $1/k_p''(\omega)$, at which its amplitude decreases. For the surface impedance in the frequency range (27) we obtain

$$Z(\omega) = \frac{\omega}{\sqrt{\omega^2-\omega_L^2}} - \frac{i}{2}\left(\frac{\alpha}{3}+1\right)\frac{\nu\,\omega_L^2}{\left(\omega^2-\omega_L^2\right)^{3/2}}. \tag{29}$$

The absorption coefficient (7) of the incident wave in the frequency range (27) can be represented as

$$A(\omega) \approx \frac{4\omega\sqrt{\omega^2-\omega_L^2}}{\left(\omega+\sqrt{\omega^2-\omega_L^2}\right)^2}. \tag{30}$$

As can be seen from (30) $A(\omega)$ in the linear approximation does not depend on the collision frequency of photoelectrons.

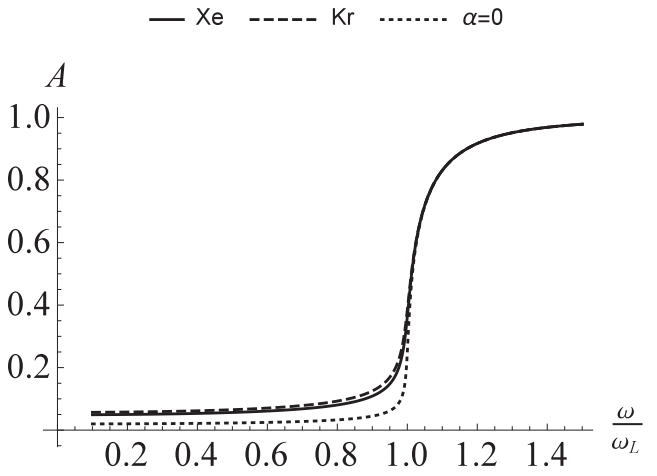

FIG. 5. Dependence of the absorption coefficient $A(\omega)$ on the incident field frequency ω.

With increasing ω the absorption coefficient (30) tends to unity in accordance with the asymptotic formula $A(\omega) \approx 1 - \omega_L^4/16\omega^4$, $\omega \gg \omega_L$. The described behavior of $A(\omega)$ reflects the fact that in the frequency region (27) almost all the energy of the incident wave passes into the plasma, leading to the excitation of an electromagnetic wave weakly attenuated in space.

Figure 5 shows the absorption coefficient for the considered frequency range of the incident radiation, taking into account the dependence of the electron collision frequency on their energy (solid and dashed curves) and without it (dotted curve). For Fig. 5 the values $\nu = 0.01\omega_L$, $\alpha \approx 4.47$ for Xe, and $\alpha \approx 5.78$ for Kr were used. Such α values correspond to the average photoelectron energies $\epsilon_0 = 2.87$ eV and $\epsilon_0 = 2$ eV, respectively. The average energies were obtained from the multiphoton photoelectric effect formula. Three-photon ionization was chosen for xenon at photon energy $\hbar\Omega = 5$ eV; four photon was chosen for krypton at photon energy $\hbar\Omega = 4$ eV.

VI. NORMAL SKIN EFFECT

We consider the case when the collision frequency of electrons with neutral atoms satisfies the inequalities

$$\nu \gg \omega, kv_0. \tag{31}$$

Under these conditions, the permittivity (5) has the form

$$\varepsilon_{\rm tr}(\omega) = 1 - \frac{\omega_L^2}{(\omega+i\nu)^2}\left[1+i\left(1-\frac{\alpha}{3}\right)\frac{\nu}{\omega}\right] \simeq 1 + \frac{\omega_L^2}{\nu^2}\left[1+2i\frac{\omega}{\nu}+i\left(1-\frac{\alpha}{3}\right)\frac{\nu}{\omega}\right]. \tag{32}$$

The presence of an additional coefficient $1-\alpha/3$ allows us to consider two different limiting cases. If, along with the inequalities (31), the condition

$$\nu(1-\alpha/3) \gg \omega \tag{33}$$

is satisfied, then the transverse permittivity (32) can be represented as

$$\varepsilon_{\rm tr}(\omega) = 1 + i\Big(1 - \frac{\alpha}{3}\Big)\frac{\omega_L^2}{\omega\nu} \tag{34}$$

characteristic of a normal skin effect. As can be seen from Fig. 4(a), for xenon the values of α, for which the range (33) is realized, lie in the range of energies less than 0.5 eV and greater than 4 eV. For krypton [see Fig. 4(b)] the values of α, satisfying the condition (33), correspond to electron energies less than 0.5 eV and greater than 5 eV. The electrons distribution of the form (1) with energies greater than 4 eV or 5 eV can be realized by ionizing the gas with ultraviolet radiation. The range of energies below 0.5 eV requires additional consideration, since at such low energies the function (1) poorly approximates the photoelectron distribution. The solution of Eq. (9) corresponding to the formula (34) lies in the first quarter of the complex wave number and, for collision frequencies in the range $(1-\alpha/3)\omega_L^2 \gg \omega\nu$, has the form

$$k_p c \approx \frac{1+i}{\sqrt{2}}\sqrt{(1-\alpha/3)\frac{\omega}{\nu}}\omega_L. \tag{35}$$

In this case, the field $E_1(z)$ is given by the expression (15), in which the term containing $(v_0\omega_L/\omega c)^2$ is omitted. The contribution to the full field from $E_2(z)$ (11) is less than from $E_1(z)$, if the parameter $(v_0\omega_L/c\nu)^3(\omega/\nu)^{3/2}\sqrt{1-\alpha/3}$ is small. The surface impedance can be written as

$$Z(\omega) = \frac{1-i}{\sqrt{2}}\frac{\sqrt{\nu\omega}}{\omega_L}\frac{1}{\sqrt{1-\alpha/3}}. \tag{36}$$

The absorption coefficient (7) corresponding to the impedance (36) has the form

$$A(\omega) \approx \sqrt{\frac{8\nu\omega}{\omega_L^2}}\frac{1}{\sqrt{1-\alpha/3}}. \tag{37}$$

Then, when $1 > 1-\alpha/3 > \omega/\nu$, due to the Ramsauer-Townsend effect, the absorption increases $1/\sqrt{1-\alpha/3}$ times.

VII. PHOTOIONIZED PLASMA—DIELECTRIC

As can be seen from Fig. 4, in inert gases there is the possibility of realizing the conditions in which

$$\nu \gg \omega \gg \nu(1-\alpha/3) > 0. \tag{38}$$

For example, for Xe this possibility is realized at energies close to ~0.5 eV or ~3.5 eV [see Fig. 4(a)], and for Kr at energies close to ~0.5 eV or ~4.5 eV [see Fig. 4(b)]. Under these conditions, the transverse permittivity has the form

$$\varepsilon_{\rm tr}(\omega) = \varepsilon' + i\varepsilon'' = 1 + \frac{\omega_L^2}{\nu^2}\Big[1 + 2i\frac{\omega}{\nu} + i\Big(1-\frac{\alpha}{3}\Big)\frac{\nu}{\omega}\Big], \tag{39}$$

where $\varepsilon' = 1 + \omega_L^2/\nu^2$ is much greater than $\varepsilon'' = (\omega_L^2/\nu^2)[(1-\alpha/3)\nu/\omega + 2\omega/\nu]$. The response of a photoionized plasma to radiation with a frequency ω from the interval (38) is similar to the response of a dielectric. In this case, the value of the pole k_p lies close to the real axis of the complex wave number plane and has the form

$$k_p c \cong \omega\sqrt{\varepsilon'}\Big(1 + i\frac{\varepsilon''}{2\varepsilon'}\Big). \tag{40}$$

The scale of spatial oscillations is $\sim c/\omega\sqrt{\varepsilon'}$ and significantly less than the distance $2(c/\omega)\sqrt{\varepsilon'}/\varepsilon''$, at which the amplitude of the electric field decays. From the surface impedance definition it follows that

$$Z(\omega) \cong \frac{1}{\sqrt{\varepsilon'}}\Big(1 - i\frac{\varepsilon''}{2\varepsilon'}\Big). \tag{41}$$

Substituting the obtained impedance (41) into the expression for the absorption coefficient (7), we obtain

$$A(\omega) \cong \frac{4\sqrt{\varepsilon'}}{(1+\sqrt{\varepsilon'})^2} = \frac{4\nu\sqrt{\nu^2+\omega_L^2}}{\big(\nu+\sqrt{\nu^2+\omega_L^2}\big)^2}. \tag{42}$$

For $\nu \ll \omega_L$ the absorption coefficient is proportional to the collision frequency and increases to unity at $\nu \gg \omega_L$.

VIII. DISCUSSION

Let us discuss some of the conditions under which the above described regularities of probe radiation interaction with photoionized plasma can be observed. Since the properties of plasma formed during the ionization of argon and xenon atoms differ slightly, let us limit ourselves to the estimates for xenon. We assume that under the influence of a short pulse of laser radiation on the gas xenon with density of atoms $N = 2.5\times10^{17}$ cm^{-3} a weakly ionized gas with the energy of photoelectrons $\varepsilon_0 = 2.87$ eV and the degree of ionization 10^{-3} is formed due to multiphoton ionization. The density of ions and photoelectrons is $n = 2.5\times10^{14}$ cm^{-3} and the characteristic photoelectron velocity is $v_0 = (2\varepsilon_0/m)^{1/2} = 10^8$ cm/s. Under these conditions, the plasma frequency of electrons is $\omega_L = 0.9\times10^{12}$ s^{-1}, the effective frequency of electron elastic collisions with neutral atoms according to Fig. 1 is equal to $\nu = 4\times10^{10}$ s^{-1}, and the parameter α according to Fig. 4(a) is 4.47. For comparison, the frequencies of electron-electron ν_{ee} and electron-ion ν_{ei} collisions are given below. Since ions are single ionized, $\nu_{ee} = \nu_{ei} = 4\pi e^4 n\Lambda/m^2 v_0^3 = 1.5\times10^9$ s^{-1}. In this estimation for the Coulomb logarithm the ratio $\Lambda = \ln(\varepsilon_0 v_0/\omega_L e^2) = 7.7$ is used. The frequency of electron inelastic collisions with neutral Xe atoms is even less: $\nu_\varepsilon = (2m/M)\nu = 3.3\times10^5$ s^{-1}. Under the above conditions, after rapid multiphoton ionization of the Xe atoms in the time range from $1/\nu = 25$ ps and up to $1/\nu_{ee} = 0.65$ ns, there is a plasma with nonequilibrium distribution of photoelectrons of the form (1). If such a plasma is exposed to radiation with the frequency $\omega = 0.5\times10^{12}$ s^{-1}, i.e., approximately 0.1 THz, then the inequalities (12) and (18) are satisfied, because $\nu \ll \omega$ as well as $kv_0 = (v_0/c)\omega_L = 0.3\times10^{10}$ s$^{-1} \ll \omega$ and $(\nu/4)(1+\alpha/3) = 2.5\times10^{10}$ s$^{-1} \ll \omega_L - \omega = 0.4\times10^{12}$ s^{-1}. In this case the absorption coefficient of terahertz radiation $A = 25\%$, according to (21). Due to the Ramsauer-Townsend effect, the absorption coefficient has increased by 2.5 times. Slightly different absorption conditions are implemented at test radiation frequency equal to 0.15 THz, that is, at $\omega = \omega_L$. In this case, the inequalities (12) are still

satisfied, as the frequency has increased and the characteristic wave number k has decreased [see ratio (24)]. Instead of the inequality (18), the reverse inequality (23) is now realized and the absorption coefficient is described by the expression (26). For the above parameters the absorption coefficient is equal to $A = 94\%$. Due to the Ramsauer-Townsend effect, there was a relative increase of absorption by a factor of 1.6. The above estimates relate to the conditions under which the mode of high-frequency skin-effect is implemented.

Now let us consider the conditions when we can speak about a normal skin effect. At atmospheric pressure, the density of xenon atoms is $N = 2.5 \times 10^{19}$ cm^{-3}. We assume that due to multiphoton ionization of Xe a weakly ionized gas with the density of ions and electrons $n = 2.5 \times 10^{16}$ cm^{-3} and the characteristic energy of photoelectrons $\varepsilon_0 = 5$ eV was formed. In this case, $\alpha = 1.5$, according to Fig. 4(a), and the elastic collision frequency of photoelectrons with Xe atoms is $\nu = 9 \times 10^{12}$ s^{-1}, according to Fig. 1(a). The electron-electron collision frequency is $\nu_{ee} = 5.4 \times 10^{10}$ s^{-1} and plasma frequency is $\omega_L = 9 \times 10^{12}$ s^{-1}. Under these conditions in the time range from $1/\nu = 0.1$ ps and up to $1/\nu_{ee} = 18$ ps the distribution of photoelectrons is described by the expression (1). When such a plasma is exposed to probe radiation with a frequency $\omega = 0.5 \times 10^{12}$ s^{-1}, the normal skin-effect mode is realized, since the conditions (31) and (33) are satisfied. The wave number described by the formula (35) should be used when the condition (31) is checked. As a result, for the absorption coefficient of the terahertz range radiation according to the ratio (37) we have the estimate $A = 94\%$. Due to the Ramsauer-Townsend effect the absorption coefficient has increased by 1.4 times.

Another of the above-mentioned modes of test radiation interaction with photoionized inert gas plasma is realized under the conditions when, as before, the density of xenon atoms is $N = 2.5 \times 10^{19}$ cm^{-3} and the density of ions and electrons is $n = 2.5 \times 10^{16}$ cm^{-3}. However, the energy of photoelectrons is so close to the value $\varepsilon_0 = 4$ eV that the parameter α almost does not differ from 3 [see Fig. 4(a)]. When $\alpha = 3$, inequalities (38) are easily achievable with a proper selection of the probe radiation frequency. Under these conditions, as before, $\omega_L = 9 \times 10^{12}$ s^{-1}, but the collision frequencies of photoelectrons are different. According to Fig. 1(a) at $\varepsilon_0 = 4$ eV for the elastic collision frequency of photoelectrons we have $\nu = 8 \times 10^{12}$ s^{-1}. The frequency of electron-electron collisions is slightly higher than in the case described above $\nu_{ee} = 7.1 \times 10^{10}$ s^{-1}. The time range in which the photoelectron distribution (1) is implemented is quite wide: from $1/\nu = 0.13$ ps to $1/\nu_{ee} = 14$ ps. The influence of spatial dispersion, as can be seen from the ratio (40), as before, is insignificant. Under these conditions, the response of photoionized plasma to terahertz radiation, for example, with a frequency $\omega = 2 \times 10^{12}$ s^{-1} (i.e., 0.3 THz) is similar to the response of a dielectric which, according to the ratio (39), has a dielectric constant of $\varepsilon' + i\varepsilon'' = 2.3 + i0.63$. Finally, for the absorption coefficient described by the expression (42), we have the estimate $A = 96\%$.

It can be seen from the presented discussion that the features of the probe radiation interaction with photoionized inert gas plasma having atmospheric pressure or close to it are of interest for the study of the terahertz frequency range. At the ionization of a highly rarefied noble gas, a plasma with a lower density of photoelectrons is formed. As a result, the plasma frequency and electron collision frequencies are reduced. In such conditions, the above described interaction features of the test radiation are realized in the microwave range, or at even lower frequencies.

IX. CONCLUSIONS

The features of the monochromatic wave penetration into a semibounded plasma obtained as a result of multiphoton ionization of inert gas atoms are studied above. An expression for the permittivity of such a plasma is obtained. The main feature of this expression is the parameter α—a value determined by the average photoelectron energy and the type of energy dependence of the scattering transport cross section. The plasma field is represented in the form of two terms. The first of them arises from the pole in the upper half-plane of the complex wave number and the second corresponds to the contribution from the banks of the cut in the same half-plane. Under the conditions of the high-frequency skin effect, when the role of spatial dispersion is small, the second contribution is less than the first by $\sim v_0^2\omega_L^2/c^2\omega^2$ times. Expressions for the surface impedance and absorption coefficient in different frequency ranges of the probe wave are obtained: when the frequency is not close to Langmuir frequency, close to Langmuir frequency, and exceeds Langmuir frequency. Field absorption is mainly determined by collisions of photoelectrons with atoms. For frequencies noticeably lower than the Langmuir frequency, the field decays at a distance $\sim c/\sqrt{\omega_L^2 - \omega^2}$, and the absorption coefficient linearly depends on the collision frequency. When the field frequency approaches Langmuir's one, the effective penetration depth is inversely proportional to $\sqrt{\nu}$ and turns out to be significantly larger than in the low-frequency case. The absorption also increases and depends on the frequency of collisions like $\sqrt{\nu}$. Taking into account the Ramsauer-Townsend effect leads to an increase in absorption over the entire range of frequencies under consideration by $(\alpha/3 + 1)$ times. With a further increase in the frequency, the length of the transverse electromagnetic wave propagating in the plasma becomes much smaller than the characteristic scale of its amplitude attenuation. The absorption coefficient ceases to depend on the collision frequency in the linear approximation and tends to unity. The low-frequency field penetration in the normal skin-effect mode is described. It is shown that in this mode the absorption coefficient increases by $1/\sqrt{1 - \alpha/3}$ times. Finally, conditions are found under which the properties of a photoionized plasma are similar to those of a dielectric with a positive real part of the permittivity $\varepsilon' = 1 + \omega_L^2/\nu^2$ and a small positive imaginary part $\varepsilon'' \ll \varepsilon'$. The possibility of realizing the field penetration regimes described above depends on the ratio of the field frequency ω, the collision frequency of photoelectrons ν, their plasma frequency ω_L, and how the photoionized plasma is created. The last one is due to the fact that the characteristic energies of photoelectrons are set during multiphoton ionization and the derivative of the effective frequency of photoelectron collisions with inert gas atoms depends on these energies.

[1] T. Marchenko, H. G. Muller, K. J. Schafer, and M. J. J. Vrakking, Wavelength dependence of photoelectron spectra in above-threshold ionization, J. Phys. B: At., Mol., Opt. Phys. **43**, 185001 (2010).

[2] P. A. Korneev, S. V. Popruzhenko, S. P. Goreslavski, T.-M. Yan, D. Bauer, W. Becker, M. Kübel, M. F. Kling, C. Rödel, M. Wünsche, and G. G. Paulus, Interference Carpets in Above-Threshold Ionization: From the Coulomb-Free to the Coulomb-Dominated Regime, Phys. Rev. Lett. **108**, 223601 (2012).

[3] M. Li, Y. Liu, H. Liu, Y. Yang, J. Yuan, X. Liu, Y. Deng, C. Wu, and Q. Gong, Photoelectron angular distributions of low-order above-threshold ionization of Xe in the multiphoton regime, Phys. Rev. A **85**, 013414 (2012).

[4] H. Liu, Y. Liu, L. Fu, G. Xin, D. Ye, J. Liu, X. T. He, Y. Yang, X. Liu, Y. Deng, C. Wu, and Q. Gong, Low Yield of Near-Zero-Momentum Electrons and Partial Atomic Stabilization in Strong-Field Tunneling Ionization, Phys. Rev. Lett. **109**, 093001 (2012).

[5] M. Li, J.-W. Geng, H. Liu, Y. Deng, C. Wu, L.-Y. Peng, Q. Gong, and Y. Liu, Classical-Quantum Correspondence for Above-Threshold Ionization, Phys. Rev. Lett. **112**, 113002 (2014).

[6] M. Li, P. Zhang, S. Luo, Y. Zhou, Q. Zhang, P. Lan, and P. Lu, Selective enhancement of resonant multiphoton ionization with strong laser fields, Phys. Rev. A **92**, 063404 (2015).

[7] L. Zhang, Z. Miao, W. Zheng, X. Zhong, and C. Wu, Nonresonant multiphoton ionization of xenon atoms by femtosecond laser pulses, Chem. Phys. **523**, 52 (2019).

[8] G. Petite, P. Agostini, and F. Yergeau, Intensity, pulse width, and polarization dependence of above-threshold-ionization electron spectra, JOSA B **4**, 765 (1987).

[9] H. G. Muller, H. B. van Linden van den Heuvell, P. Agostini, G. Petite, A. Antonetti, M. Franco, and A. Migus, Multiphoton Ionization of Xenon with 100-fs Laser Pulses, Phys. Rev. Lett. **60**, 565 (1988).

[10] H.-P. Kang, C.-L. Wang, Z.-Y. Lin, Y.-J. Chen, M.-Y. Wu, W. Quan, H.-P. Liu, and X.-J. Liu, Intensity and polarization effects in short-pulse multiphoton ionization of xenon, Chin. Phys. Lett. **28**, 083201 (2011).

[11] I. Barth and O. Smirnova, Spin-polarized electrons produced by strong-field ionization, Phys. Rev. A **88**, 013401 (2013).

[12] A. Hartung, F. Morales, M. Kunitski, K. Henrichs, A. Laucke, M. Richter, T. Jahnke, A. Kalinin, M. Schöffler, L. P. H. Schmidt, M. Ivanov, O. Smirnova, and R. Dörner, Electron spin polarization in strong-field ionization of xenon atoms, Nat. Photon. **10**, 526 (2016).

[13] M.-M. Liu, Y. Shao, M. Han, P. Ge, Y. Deng, C. Wu, Q. Gong, and Y. Liu, Energy- and Momentum-Resolved Photoelectron Spin Polarization in Multiphoton Ionization of Xe by Circularly Polarized Fields, Phys. Rev. Lett. **120**, 043201 (2018).

[14] N. B. Delone and V. P. Krainov, Energy and angular electron spectra for the tunnel ionization of atoms by strong low-frequency radiation, J. Opt. Soc. Am. B **8**, 1207 (1991).

[15] K. Vagin and S. Uryupin, Amplification of short pulse passing through anisotropic plasma layer, Phys. Lett. A **379**, 747 (2015).

[16] N. B. Delone and V. P. Krainov, Tunneling and barrier-suppression ionization of atoms and ions in a laser radiation field, Phys. Usp. **41**, 469 (1998).

[17] K. Vagin, T. Mamontova, and S. Uryupin, High-frequency waves in plasma formed as a result of tunnel ionization of atoms by circularly polarized radiation, Phys. Lett. A **381**, 2350 (2017).

[18] A. Bogatskaya and A. Popov, On the possibility of the amplification of subterahertz electromagnetic radiation in a plasma channel created by a high-intensity ultrashort laser pulse, JETP Lett. **97**, 388 (2013).

[19] K. Vagin, T. Mamontova, and S. Uryupin, Waves in plasma formed by above-threshold ionization of gas atoms, Phys. Lett. A **383**, 2897 (2019).

[20] K. Y. Vagin and S. A. Uryupin, Collective modes of plasma formed by multiphoton ionization of rarefied gas, Plasma Sources Sci. Technol. **29**, 035005 (2020).

[21] V. Y. Bychenkov and V. Tikhonchuk, Instabilities and generation of electromagnetic waves in plasma produced by a short high-power laser pulse, Laser Phys. **2**, 525 (1992).

[22] M. G. Haines, Magnetic-field generation in laser fusion and hot-electron transport, Can. J. Phys. **64**, 912 (1986).

[23] V. Y. Bychenkov, D. V. Romanov, W. Rozmus, C. E. Capjack, and R. Fedosejevs, Distinctive features of photoionized plasma from short x-ray-pulse interaction with gaseous medium, Phys. Plasmas **13**, 013101 (2006).

[24] I. Andriyash, V. Bychenkov, and W. Rozmus, Evolution of photoionization two-stream instability in collisional plasma, High Energy Density Phys. **4**, 73 (2008).

[25] K. Vagin and S. Uryupin, Amplification of electromagnetic radiation by a nonequilibrium plasma unstable against the development of Weibel instability, JETP **111**, 670 (2010).

[26] P. Agostini and G. Petite, *Atomic and Molecular Processes with Short Intense Laser Pulses* (Plenum Press, New York, 1988), pp. 135–143.

[27] K. Vagin, T. Mamontova, and S. Uryupin, Longitudinal electron waves in plasma formed at multi-photon ionization of atoms by a short laser pulse, Contrib. Plasma Phys. **58**, 276 (2018).

[28] J. Townsend and V. Bailey, XCVII. The motion of electrons in gases, London, Edinburgh, Dublin Philos. Mag. J. Sci. **42**, 873 (1921).

[29] C. Ramsauer, Über den wirkungsquerschnitt der gasmoleküle gegenüber langsamen elektronen, Ann. Phys. (Leipzig) **369**, 513 (1921).

[30] R. B. Brode, The quantitative study of the collisions of electrons with atoms, Rev. Mod. Phys. **5**, 257 (1933).

[31] A. Bogatskaya, I. Smetanin, E. Volkova, and A. Popov, Guiding and amplification of microwave radiation in a plasma channel created in gas by intense ultraviolet laser pulse, Laser Part. Beams **33**, 17 (2015).

[32] Bibliography of electron and photon cross sections with atoms and molecules published in the 20th century—xenon, National Institute for Fusion Research, research report NIFS-data series, NIFS-data, 79th ed., 2003.

[33] J. L. Pack, R. E. Voshall, A. V. Phelps, and L. E. Kline, Longitudinal electron diffusion coefficients in gases: Noble gases, J. Appl. Phys. **71**, 5363 (1992).

[34] V. P. Silin and A. A. Rukhadze, *Electromagnetic Properties of Plasma and Plasma-Like Media (in Russian)* (Gosatomizdat, Moscow, 1961).

[35] M. Abramowitz and I. A. Stegun, *Handbook of Mathematical Functions with Formulas, Graphs, and Mathematical Tables* (Dover, New York, 1964).

[36] K. Vagin, T. Mamontova, and S. Uryupin, Penetration of electromagnetic radiation in plasma produced by multiphoton ionization, J. Russ. Laser Res. **40**, 474 (2019).